

Research & Reviews: Journal of Pure and Applied Physics

Study of Room Temperature Ferromagnetic And Dielectric Properties in the Composites of $\text{Fe}_{1.2}\text{Ga}_{0.8}\text{O}_3$ and $\text{Co}_{1.25}\text{Fe}_{1.75}\text{O}_4$ Oxides

Vijayasri G and Bhowmik RN*

¹Department of Physics, Pondicherry University, R.V. Nagar, Kalapet, Pondicherry-605014, India.

Research Article

Received date: 06/23/2015

Accepted date: 07/26/2015

Published date: 07/28/2015

*For Correspondence

Bhowmik RN, Department of Physics, Pondicherry University, R.V. Nagar, Kalapet, Pondicherry-605014, India. Tel: +91-9944064547; Fax: +91-413-2655734

E-mail: rnbhowmik.phy@pondiuni.edu.in

Keywords: Magnetic composite, Interfacial coupling, Magnetic Properties, Dielectric properties.

ABSTRACT

The composites of $\text{Fe}_{1.2}\text{Ga}_{0.8}\text{O}_3$ (metal doped hematite) and $\text{Co}_{1.25}\text{Fe}_{1.75}\text{O}_4$ (spinel ferrite) have been prepared by weight mixing method. X-ray diffraction pattern and Raman spectroscopy have been used to confirm the coexistence of rhombohedral structure of $\text{Fe}_{1.2}\text{Ga}_{0.8}\text{O}_3$ and spinel structure of $\text{Co}_{1.25}\text{Fe}_{1.75}\text{O}_4$. The Energy dispersive analysis of X-ray spectrum has been used to determine elemental composition of the composite samples. The ferromagnetic and dielectric properties of the material have been studied at room temperature by adjusting weight ratio of $\text{Fe}_{1.2}\text{Ga}_{0.8}\text{O}_3$ and $\text{Co}_{1.25}\text{Fe}_{1.75}\text{O}_4$ components. The samples have shown properties of ferromagnetic-dielectric material with electrical conductivity 10^{-8} – 10^{-11} S/cm, dielectric constant in the range 0.002-20 and extremely low dielectric loss (<1) above 1 kHz. The composite samples showed good signature of ferroelectric properties, although polarization leakage has increased in the composite samples with the increase of $\text{Fe}_{1.2}\text{Ga}_{0.8}\text{O}_3$ content. The results could be interesting for designing suitable ferromagnetic and ferroelectric composite materials for possible applications in spintronics devices, whose operation can be controlled by simultaneous applications of electric field and magnetic field

INTRODUCTION

The composite materials with variable ferromagnetic and ferroelectric properties have received recent attention for fundamental study of magneto-electric effect and applications in modern electromagnetic devices, e.g., filters, chip inductors and capacitors [1,2]. The material with coexisting ferroelectric and magnetic orders and having strong electro-magnetic coupling in single phased crystal structure is naturally rare [3]. This limits the technological applications of magnetic spinel oxides. Alternatively, hybrid magnetic composites have been designed by suitable admixture of ferromagnetic component (spinel oxide) and ferroelectric component (e.g., BaTiO_3) in order to enhance the electro-magnetic coupling in the material [4]. Recently, metal (Al, Ti, Ga) doped hematite ($\alpha\text{-Fe}_2\text{O}_3$) have shown many interesting electro-magnetic properties that are useful in spintronic devices [5,6]. The magnetic and dielectric properties in metal doped hematite are found to be well advanced in comparison to pure hematite system [5,7]. The electro-magnetic properties in metal doped $\alpha\text{-Fe}_2\text{O}_3$ system depend on the modification in rhombohedral planes of the crystal structure [8]. Ga doped hematite system has exhibited room temperature ferromagnetism, extremely low dielectric loss, and semiconductor properties with optical band gap in the range 2.4-2.5 eV [5,7,9]. Being canted (anti) ferromagnet, magnetic moment per formula unit of the Ga doped hematite system at room temperature is low, typically 0.02-0.03 $\mu\text{B}/\text{Fe}$ atoms [5] and the ferromagnetic moment per Fe atom in Ga doped hematite decreases on decreasing temperature below room temperature due to dominance of antiferromagnetic state of the system [7]. On the other hand, magnetic moment per Fe atom in Co ferrite can be designed greater than 1 μB and magnetic moment in Co doped spinel ferrites generally increased below room temperature due to their typical ferro/ferrimagnetic properties [10]. Magnetic squareness and coercivity are greatly varied depending on the Co content in spinel ferrite structure. Co ferrites also exhibited good dielectric properties with low dielectric loss, moderate dielectric constant

and signature of (multi)ferroelectricity [11-13]. Hence, there is a large scope of tuning magnetic moment and dielectric parameters in the composites of Ga doped hematite and Co ferrite.

In this work, we report the room temperature magnetic and dielectric properties in the composites of Ga doped hematite ($\text{Fe}_{1.2}\text{Ga}_{0.8}\text{O}_3$) and Co ferrite ($\text{Co}_{1.25}\text{Fe}_{1.75}\text{O}_4$) samples. Our main objective is to study the variation of magnetic and dielectric properties in the prepared magnetic composite samples due to modified magnetic exchange coupling at the interfaces of two different types of magnetic particles.

EXPERIMENTAL

The composites have been prepared by mixing specific weight ratio of $\alpha\text{-Fe}_{1.2}\text{Ga}_{0.8}\text{O}_3$ (rhombohedral phase) and $\text{Co}_{1.25}\text{Fe}_{1.75}\text{O}_4$ (cubic spinel structure). The starting materials $\alpha\text{-Fe}_{1.2}\text{Ga}_{0.8}\text{O}_3$ and $\text{Co}_{1.25}\text{Fe}_{1.75}\text{O}_4$ have been prepared separately. Single phased structure of the individual component has been confirmed before mixing to form the composite material. The mixture of two components has been ground for 2 hrs in air. Finally, the composite powder has been made into pellets and the pellets have been annealed at 800°C for 8 hrs under high vacuum. The annealing of the composites has been performed under vacuum by considering the fact that stabilization of rhombohedral structure in $\alpha\text{-Fe}_{1.2}\text{Ga}_{0.8}\text{O}_3$ needs high vacuum condition [5, 7]. The composite samples have been prepared for the mixed weight ratio of $\text{Fe}_{1.2}\text{Ga}_{0.8}\text{O}_3$ (GF) and $\text{Co}_{1.25}\text{Fe}_{1.75}\text{O}_4$ (CF) ferrite at 1:3, 2:2, and 3:1, and the corresponding samples have been denoted as Ga_1Co_3 , Ga_2Co_2 and Ga_3Co_1 , respectively.

Crystalline structure of the composites has been studied by using X-ray diffraction (XRD) pattern and Raman spectroscopy at room temperature. The XRD pattern has been recorded in the 2θ range 20-70° with step size 0.02° using CuK_α radiation using X-ray diffractometer (X-Pert PANalytical). Raman spectra of the samples have been recorded using Raman microscope (Reni Shaw, UK) with 514 nm LASER. LASER power has been optimised to 3 mW on the sample surface for acquisition time 30 s. Surface morphology of the samples has been studied using Scanning Electron Microscope (HITACHI S- 3400 N). Elemental composition of the samples has been checked by energy dispersive analysis of X-ray (EDX) spectrometer (Thermo electron corporation Instrument, USA). Magnetic property of the samples has been measured using low field (± 15 kOe) vibrating sample magnetometer (Lakeshore 7404). Dielectric spectrometer (Novo control Technology, Germany) with Alpha-analyzer has been used for measurement of the dielectric properties at voltage amplitude 1 V in the frequency range 1 Hz-10 MHz. The disc-shaped samples ($\varnothing \sim 12$ mm, thickness ~ 1 mm) have been sandwiched between two gold-coated plates. The plates have been connected to the spectrometer with shielded cables. Electric field dependence of polarization of the samples has been measured at frequency 1 kHz using P-E loop tester (Radiant Tech., USA).

RESULTS AND DISCUSSION

Structural Properties

XRD pattern of the composite samples in **Figure 1** confirms the presence of $\text{Fe}_{1.2}\text{Ga}_{0.8}\text{O}_3$ (GF) and $\text{Co}_{1.25}\text{Fe}_{1.75}\text{O}_4$ (CF) without forming any additional phase. FULLPROF program has been used to analyze XRD patterns of the composites. XRD profile of the composite samples matched to mixed phases of rhombohedral structure with $R\bar{3}C$ space group for $\alpha\text{-Fe}_{1.2}\text{Ga}_{0.8}\text{O}_3$ and cubic spinel structure with $Fd3m$ space group for $\text{Co}_{1.25}\text{Fe}_{1.75}\text{O}_4$ [10, 14]. The variation of major peaks height ratio between Co ferrite (311 peak at $2\theta \sim 35.65^\circ$) and Ga doped hematite (104 peak at $2\theta \sim 33.25^\circ$) is well consistent to their weight ratio in the composite. The lattice parameters (a, c) and cell volume (V) of the samples have been shown in **Table 1**. The lattice parameters and volume of the components in composite materials showed minor changes with respect to the lattice parameters in parent compounds before making composite. The coexisting phases may be affecting the interfacial lattice structure in composite samples and broadening in the peak width. The grain size $\langle d \rangle$ and root mean square lattice strain (ϵ_{rms}) of the samples have been calculated using Williamson-Hall equation [15] $\beta_L = 0.89\lambda / (\langle d \rangle \cos\theta_c)$ and $\beta_G^2 = 8\pi(\tan^2\theta_c)(\epsilon_{\text{rms}})^2$, respectively. The β_L and β_G are the Lorentzian and Gaussian components (β hkl is full width at half maximum of intensity in degree) and λ (1.5405 Å) is the wavelength of x-ray radiation. The grain (crystallite) size of samples have been calculated for predominant intense XRD peaks by fitting each peak profile to a pseudo-Voigt function, consisting of Lorentzian and Gaussian components. The Lorentzian component has been attributed to grain size ($\langle d \rangle$) and the Gaussian component has been attributed to lattice strain (ϵ_{rms}) of the samples. We observed a decreasing trend of grain size, while an increasing trend of lattice strain with the increase of GF component in the composite samples.

Surface morphology of the particles in the composite samples has been examined using Scanning Electron Microscopic (SEM) images. SEM images in **Figure 2** show that nearly spherical shaped particles are agglomerated to form an assembly or cluster of particles. The cluster size increases with the increase of CF content in composite samples. This observation is consistent to the pattern of the grain size variation in the composite samples. This informs an increasing inter-particle (magnetic exchange) interaction at the interfaces of two different types magnetic particles, where ferromagnetic moment per gram of CF particles is larger than that in GF particles. The increasing magnetic exchange interactions at the interfaces facilitate more agglomeration of particles. The EDX spectra confirmed the presence of elements Fe, Ga, Co and O, and their atomic ratio is matched to the expected values in composite samples.

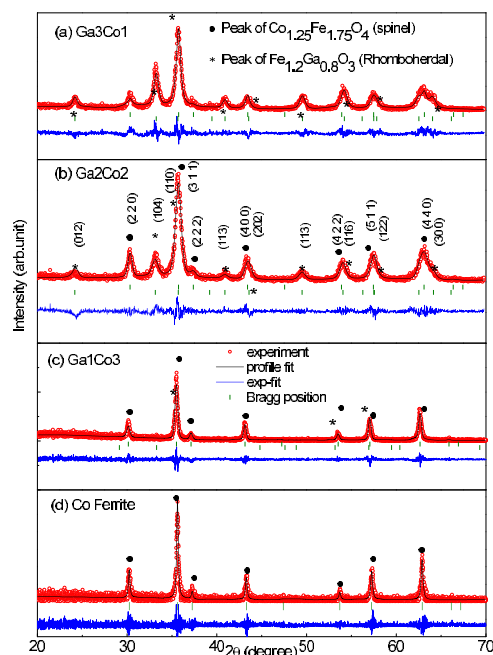


Figure 1. (Colour online) XRD pattern of the composite samples (a-c) fitted with two phase components (Ga doped hematite and Co ferrite), along with Co ferrite pattern.

Table 1. Room temperature lattice parameter, volume, grain size and strain of the composite sample calculated from XRD spectra.

| Sample | Rhombohedral with space group R3C | | | Spinel with space group Fd3m | | <d> (nm) | ε (%) |
|------------|-----------------------------------|---------------|----------------|------------------------------|----------------|----------|-------|
| | a (± 0.0002Å) | c (± 0.0006Å) | V (± 0.10(Å)³) | a (± 0.002Å) | V (± 0.10(Å)³) | | |
| Ga3Co1 | 5.06382 | 13.96591 | 310.139 | 8.40071 | 592.855 | 10 | 0.30 |
| Ga2Co2 | 5.04477 | 13.72593 | 302.521 | 8.34438 | 581.009 | 14 | 0.29 |
| Ga1Co3 | 5.03736 | 13.81199 | 303.524 | 8.34803 | 581.771 | 24 | 0.26 |
| Co Ferrite | - | - | - | 8.35255 | 582.716 | 40 | 0.08 |

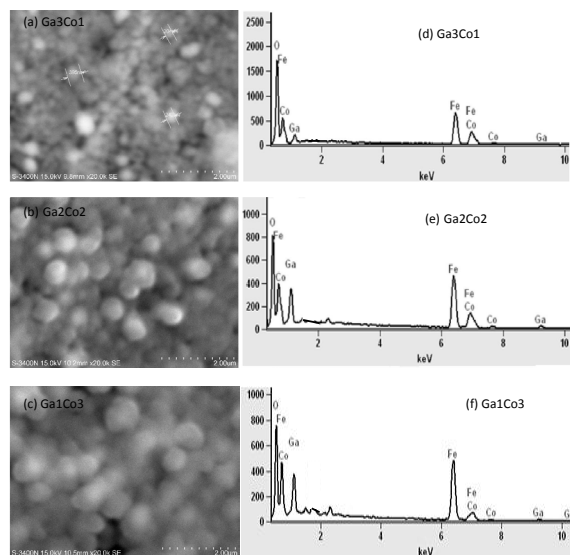


Figure 2. SEM images (a-c) and EDX spectrum (d-f) of composite samples.

Raman Analysis

Raman spectra of the samples have been recorded in the wave number range 100-1500 cm^{-1} . The Raman active phonon modes confirmed the coexistence of the rhombohedral phase of metal doped hematite and inverse spinel structure of Co ferrite [16,17]. The spectra of composite samples have shown prominent bands positions at $\sim 174 \text{ cm}^{-1}$, $\sim 224 \text{ cm}^{-1}$, $\sim 236 \text{ cm}^{-1}$, $\sim 295 \text{ cm}^{-1}$, $\sim 315 \text{ cm}^{-1}$, $\sim 411 \text{ cm}^{-1}$, $\sim 478 \text{ cm}^{-1}$, $\sim 570 \text{ cm}^{-1}$, $\sim 617 \text{ cm}^{-1}$, $\sim 682 \text{ cm}^{-1}$, and $\sim 1322 \text{ cm}^{-1}$. The identified band positions of the Raman active phonon modes corresponding to GF and CF phases are shown in **Table 2**. In **Figure 3**, we have compared the Raman spectra of the composite samples with the spectrum of pure Co ferrite. The bands at $\sim 682 \text{ cm}^{-1}$ and $\sim 617 \text{ cm}^{-1}$ have been observed in all composites. These bands are assigned to A1g(1) and A1g(2) modes representing stretching vibration of Fe^{3+} and O^{2-} ions in octahedral sites of the Co ferrite. The doublet like structure in A1g mode represents the redistribution of Fe-O and Co-O bond distance between the two sites in Co ferrite [18]. The low frequency bands at $\sim 315 \text{ cm}^{-1}$, $\sim 478 \text{ cm}^{-1}$ and $\sim 570 \text{ cm}^{-1}$

are assigned to Eg, T2g(2) and T2g(3) modes, respectively, which originated due to the tetrahedral site vibration of metal-oxygen bonds in Co ferrite. The bands in the composite samples at $\sim 224\text{ cm}^{-1}$, $\sim 236\text{ cm}^{-1}$, $\sim 295\text{ cm}^{-1}$, $\sim 315\text{ cm}^{-1}$, $\sim 411\text{ cm}^{-1}$, $\sim 478\text{ cm}^{-1}$ and $\sim 617\text{ cm}^{-1}$ are assigned due to A1g(1), Eg(1), Eg(2), Eg(3), Eg(4), A1g(2) and Eg(5) modes of the Fe-O/Ga-O vibration in rhombohedral structure of hematite^[19]. The band at 1322 cm^{-1} is a typical characteristic mode in Ga doped hematite, which arises due to magnon-magnon scattering or phonon-phonon scattering effect^[7,9]. A gradual increase of the peak intensity of the band at 1322 cm^{-1} in the composite samples is consistent to the increase of GF content.

Table 2. Peak Position (in Cm-1) for pure and different composite samples have been extracted from room temperature Raman Spectra.

| Sample | Peak Positions (cm-1) | | | | | | | | | | | |
|----------------|-----------------------|-------|-------|-------|-------|--------|--------|--------|-------|------|---------|--|
| | A1g(1) | Eg(1) | Eg(2) | Eg(3) | Eg(4) | A1g(2) | T2g(2) | T2g(3) | Eg(5) | Eu | Mgn-Mgn | |
| Fe1.2Ga0.8O3 | | | | | | | | | | | | |
| Co1.25Fe1.75O4 | T2g(1) | | | Eg | | | | | | | | |
| Ga1Co3 | 182 | - | - | 313 | 362 | 473 | 574 | 613 | 695 | 1327 | | |
| Ga2Co2 | 174 | 224 | 236 | 295 | 315 | 411 | 478 | 570 | 617 | 682 | 1322 | |
| Ga3Co1 | 182 | - | - | 313 | 362 | 472 | 574 | 613 | 695 | 1327 | | |
| Co Ferrite | 182 | - | - | 309 | 361 | 469 | 581 | 628 | 688 | - | | |

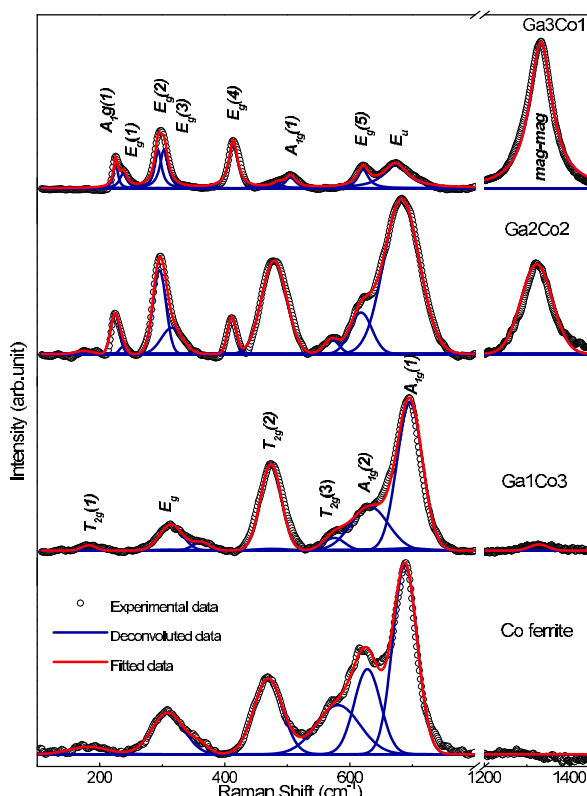


Figure 3. (Colour online) Raman spectra of the composite samples. The peaks profiles are deconvoluted with the components of Ga doped hematite and Co ferrite, along with the spectrum of Co ferrite sample.

Magnetic and ferroelectric properties

Figure 4(a) shows the magnetic field dependence of magnetization (M(H)) data at room temperature for the pure Co ferrite and composite samples. The composite samples showed ferromagnetic properties at room temperature with a clear magnetic hysteresis loop. The loop is symmetric with nearly equal magnitudes of coercivity in negative field axis (HC1) and in positive field axis (HC2). **Table 3** shows the ferromagnetic parameters, such as coercivity (HC), remnant magnetization (MR), and spontaneous magnetization (MS). The spontaneous magnetization (MS) has been derived by extrapolating the high field M(H) data on the positive magnetization (magnetic moment per gram) axis at $H = 0$. The spontaneous magnetization (MS) and coercivity for pure Co ferrite sample are $\sim 52\text{ emu/g}$ and 596 Oe , respectively. When GF is admixed with CF, the magnetization (in emu/g) first increased with the increase of less magnetic GF component. The magnetization in Ga1Co3 and Ga2Co2 composites are unusually higher than that in pure Co ferrite sample. We viewed this enhancement of magnetization in the composites as the enhancement of magnetic exchange coupling at the interfacial spin structure of ferromagnetic CF and weak ferromagnetic GF phases. The presence of a strong magnetic exchange coupling among the particles in Ga1Co3 and Ga2Co2 composite samples is also reflected in the SEM images. However, coercivity and squareness (reduced remanent magnetization with respect to spontaneous magnetization) decreased with the increase of GF component, leading to a magnetically soft phase in the composite samples. **Figure 4(b)** shows the electric field dependence of polarization (P-E) loops of the pure CF and composite samples measured at room temperature with voltage 95 V at frequency 1 kHz. The Co ferrite sample exhibited good signature of ferroelectric polarization. The polarization leakage increases in composite samples with the increase of GF component. This could be attributed to space charge polarization

effect and structural heterogeneity at the interfaces of different magnetic particles. The Ga1Co3 sample showed the best ferroelectric loop with low leakage and relatively high electrical polarization ($\sim 1.5 \times 10^{-4} \mu\text{C}/\text{cm}^2$). The ferroelectric loop shape of the Ga1Co3 composite sample is comparable to the pure Co ferrite sample. This means Ga1Co3 is the best composition for achieving good ferromagnetic and ferroelectric properties among the composite samples. The change of electrical properties in the composite samples is further understood from the dielectric measurements.

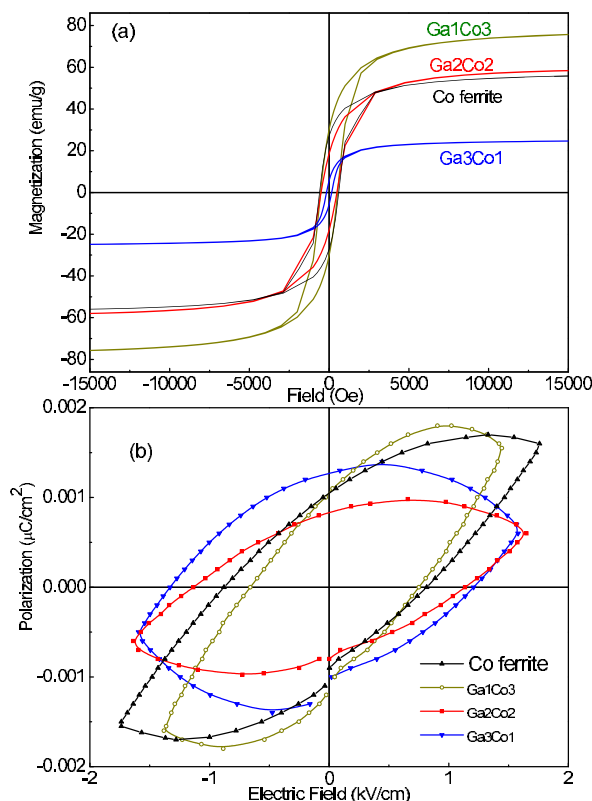


Figure 4. (Colour online) Magnetic field dependence of magnetization loop (a) and electric field dependence of polarization loop (b) for the Co ferrite and composite samples measured at room temperature.

Table 3. The calculated values of room temperature magnetic, electrical and dielectric parameters of all composites.

| Sample | Magnetic Parameters | | | | Electrical Parameters (Using Jonscher's power law and Cole-Cole plot) | | | | |
|------------|---------------------|------------|------------|-------|--|---------------------------------------|-------------------------|-----------------------------|--------|
| | HC (Oe) | MR (emu/g) | MS (emu/g) | MR/MS | ϵ' at σ_{dc} (10 ⁻⁹ S/cm) 1Hz | σ_{gb} (10 ⁻⁹ S/cm) | C (10 ⁻¹¹ F) | τ (10 ⁻⁵ S) | |
| Ga3Co1 | 163.22 | 5.72 | 22.78 | 0.25 | 5000 | 74.21 | 87.85 | 2.91 | 0.31 |
| Ga2Co2 | 492.13 | 18.35 | 54.49 | 0.34 | 450 | 2.81 | 3.41 | 3.24 | 8.45 |
| Ga1Co3 | 533.32 | 30.18 | 69.06 | 0.44 | 55 | 0.69 | 0.71 | 2.26 | 27.27 |
| Co Ferrite | 595.79 | 27.05 | 52.13 | 0.52 | 15 | 0.075 | 0.11 | 1.51 | 182.77 |

Dielectric properties

Figure 5 shows the variation of dielectric parameters (ac conductivity, dielectric constant, dielectric loss and impedance) with frequency in composite samples. The frequency (ν) dependent ac conductivity data have been fitted with equation $\sigma'(\nu) = \sigma_{dc} + \sigma'(\nu)^{[6]}$, where σ_{dc} , the dc limit of $\sigma'(\nu)$, has been estimated by extrapolating the conductivity at $\nu \rightarrow 0$ limit. The σ_{dc} showed value of the order of 10^{-12} S/cm for Co ferrite and conductivity value in the composite samples systematically increases up to the order of 10^{-7} S/cm with the increase of GF component. The dc regime of the conductivity (where σ' is nearly frequency independent) systematically extended up to the higher frequencies with the increase of GF content in the composite. The frequency activated conductivity, where conductivity rapidly increases with frequency, follows Jonscher power law: $\sigma'(\nu) = \alpha(T)\nu^n$. Here, $\alpha(T)$ is the temperature dependent parameter and n is the frequency exponent. The exponent n values have been calculated by fitting ac conductivity curves according to Jonscher power law (shown by lines in **Figure 5(a)**). The n values are 1.09, 0.88, 0.83 and 0.71 for Co Ferrite, Ga1Co3, Ga2Co2 and Ga3Co1 samples, respectively. The range of n values (0.7-1) suggests that small polaron hopping process controls the conductivity mechanism in the composite samples ^[20]. As in **Figure 5(b)**, the dielectric constant has shown an overall increase in the measurement frequency range with the increase of GF content in composite samples. **Table 3** shows that dielectric constant of the Co ferrite at 1 Hz is ~ 15 . The highest dielectric constant (~ 5000) at 1 Hz has been observed in Ga3Co1 sample. The rapid increase of dielectric constant below 1 kHz may be attributed to space charge polarization effect ^[11] at the interfaces of grains with different crystalline phase, magnetic structure and morphological difference, but dielectric constant is reasonably stable at higher frequencies. **Figure 5(c)** shows that dielectric loss ($\tan\delta$) in the composite samples is

reasonably low (0.02-30) in the frequency range 1 Hz-9 MHz, although dielectric loss is slightly increased with the increase of GF component in composite samples. This is due to good semiconductor properties of Ga doped hematite (GF) component. The relatively high conducting nature of GF component in comparison with Co ferrite component plays a significant role in the modified electrical conductivity, dielectric loss and leakage of ferroelectric polarization in composite samples. In addition to the space charge polarization, exchange of electrons between super exchange paths ($\text{Fe}^{2+}\text{-O-Fe}^{3+}$) and holes between super exchange paths ($\text{Co}^{2+}\text{-O-Co}^{3+}$) in the Co ferrite structure largely contributed to dielectric loss at lower frequencies [21]. Interestingly, dielectric loss of the composite material above 1 kHz is extremely low (<1) and it could be useful for application in electromagnetic devices. The increase of conductivity with the increase of GF component in the composite has been further understood from the analysis of impedance (Z' and Z'') data. As in **Figure 5(d)**, the real part of impedance (Z') rapidly decreases at higher frequencies and reciprocating the features in σ' (μ) data, whereas the imaginary part ($-Z''$) exhibits the properties of dielectric relaxation process. The observation of a peak in $-Z''$ vs. frequency curves (**Figure 5(e)**) suggests charge hopping mechanism between ions [22]. The hopping frequency (ω_p) shifts to higher values with the increase GF content in the composite material. A wide shift in the peak frequency from ~ 10 Hz in Co ferrite to ~ 10 kHz in Ga_3Co_1 sample suggests that not only grain boundary regime, but highly conductive grain interior also participates in dielectric properties of composite samples. The Cole-Cole plot ($-Z''$ vs. Z') of the complex impedance spectrum (**Figure 5(f)**) shows that interfacial resistance between electrode and studied material is not significant. The impedance plots are well fitted with semicircles. The resistance, contributed mainly by grain boundary resistance (R_{gb}), has been calculated from the intercept of the semi-circular arc on the Z' axis at lower frequency regime. We noted a rapid decrease of R_{gb} for the Ga_3Co_1 sample. Considering the $R||C$ circuit and applying the condition $2\pi\nu_p R_{gb} C_{gb} = 1$ at the peak position of $-Z''$ maximum of Cole-Cole plot, we found that capacitance (C_{gb}) of the composite increases with the increase of GF component. The time constant ($\tau = R_{gb} C_{gb}$) of the composite samples showed decreasing trend with the increase of GF component. Our experimental results show that GF acts as a conducting buffer for the increasing interfacial coupling between Co ferrite and Ga doped hematite (GF) grains in the composite samples. There is a large scope of varying ac conductivity, dielectric constant, dielectric loss and dielectric relaxation mechanism in the present composite materials.

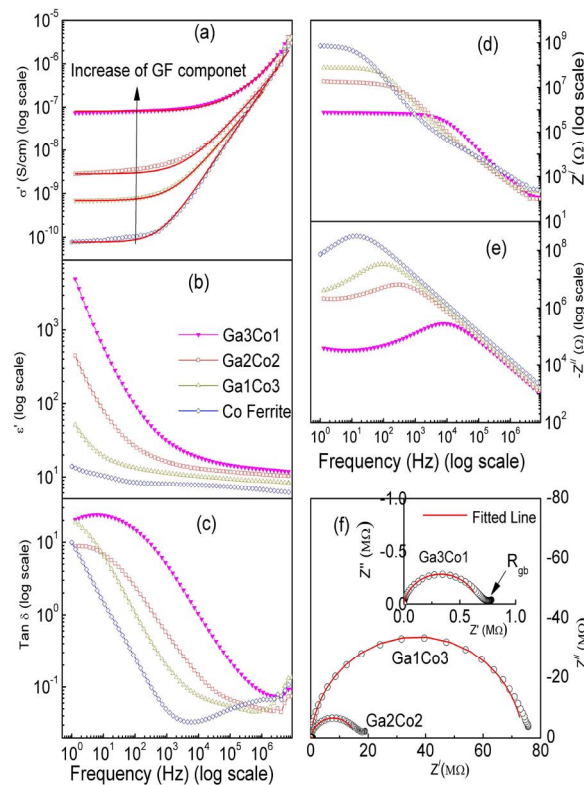


Figure 5. (Colour online) Frequency dependence of real part of ac conductivity (a), dielectric constant (b), dielectric loss (c), real part of impedance (d) and imaginary part of impedance (e) for Co ferrite and composite samples. The Cole-Cole plot ($-Z''$ vs. Z') of impedance data have been fitted with semi-circle in (f) to calculate grain boundary resistance (R_{gb}) of the samples.

CONCLUSIONS

The composite samples of $\text{Fe}_{1.2}\text{Ga}_{0.8}\text{O}_3$ (GF) and $\text{Co}_{1.25}\text{Fe}_{1.75}\text{O}_4$ (CF) oxides have been prepared. The ferromagnetic and dielectric parameters of the composites have been varied at room temperature by varying the weight ratio of the components. The electrical conductivity, dielectric parameters (dielectric constant and loss) and capacitance have increased with the increase of conductive Ga doped hematite component in the composite samples. However, higher conductivity and dielectric loss lead to higher leakage of polarization in the composite samples. Frequency dependent conductivity data indicated the semiconducting behaviour of all the samples. The Cole-Cole plot revealed that conductivity is controlled mainly by grain boundaries, but highly

conductive grains also actively participated in electrical conduction process of composite samples. The dielectric constant in composite samples has shown an overall increase in the measurement frequency range with the increase of GF content. A rapid increase of dielectric constant below 1 kHz has been attributed to space charge polarization effect at the interfaces of grains with different crystalline phase, magnetic structure and morphological differences. The dielectric constant remained stable at higher frequencies. The composite with higher ferrite content and less Ga doped hematite content (Ga_1Co_3) appeared to be the best composition for achieving higher magnetization, good signature of ferroelectric properties and moderate dielectric constant. The presented results may be relevant for the basic understanding of the magneto-electric coupling and magnetic exchange interactions at the interfaces of ferrite and metal doped hematite based semiconductors.

ACKNOWLEDGMENT

Authors thank CIF, Pondicherry University for material characterization facilities. Authors also acknowledge the research grants from DST (NO. SR/S2/CMP-0025/2011) and CSIR (No. 03(1222)/12/EMR_II), Govt. of India for continuing the research activities presented in this work.

REFERENCES

1. Patankar KK et al. Dielectric behaviour and magnetoelectric effect in $\text{CuFe}_2\text{O}_4\text{-Ba}_0.8\text{Pb}_0.2\text{TiO}_3$ composites. *Mater. Chem. Phys.* 2001; 72: 23-29.
2. Kanai T et al. A Ferroelectric Ferromagnet Composed of $(\text{PLZT})_x(\text{BiFeO}_3)_{1-x}$ Solid Solution. *Adv. Mater.* 2001; 13: 487-490.
3. Hill NA. Why Are There so Few Magnetic Ferroelectrics? *J. Phys. Chem. B.* 2000; 104: 6694-6709.
4. Ferreira NM et al. Magnetite/hematite core/shell fibres grown by laser floating zone method. *App. Surf. Sci.* 2013; 278: 203-206.
5. Naresh N and Bhowmik RN. Magnetic, dielectric and photo-absorption study of a ferromagnetic semiconductor $\alpha\text{-Fe}_{1.4}\text{Ga}_{0.6}\text{O}_3$. *AIP Advances* 2011; 1: 032121.
6. Mohapatra M and Anand S. Synthesis and applications of nano-structured iron oxides/ hydroxides – a review. *Int. J. Eng. Sci. Tech.* 2010; 2: 127-146.
7. Bhowmik RN et al. Study of low temperature ferromagnetism, surface paramagnetism and exchange bias effect in $\alpha\text{-Fe}_{1.4}\text{Ga}_{0.6}\text{O}_3$ oxide. *Current Appl. Phys.* 2014; 14: 970-979.
8. Naresh N et al. Study of surface magnetism, exchange bias effect, and enhanced ferromagnetism in $\alpha\text{-Fe}_{1.4}\text{Ti}_{0.6}\text{O}_3$ alloy. *App. Phys.* 2011; 109: 093913.
9. Lone AG and Bhowmik RN. Study of room temperature ferromagnetic and ferroelectric properties in $\alpha\text{-Fe}_{1.6}\text{Ga}_{0.4}\text{O}_3$ alloy. *J. Magn. Mater.* 2015; 379: 244-255.
10. Bhowmik RN et al. Alloying of Fe_3O_4 and Co_3O_4 to develop $\text{Co}_3\text{Fe}_3(1-x)\text{O}_4$ ferrite with high magnetic squareness, tunable ferromagnetic parameters, and exchange bias. *J. Alloys Compd.* 2013; 578: 585-594.
11. Bhowmik RN and Muthuselvam IP. Dielectric properties and signature of multi-ferroelectricity in Co_2FeO_4 : A structurally single phased and bi-phased spinel oxide. *J. Alloys. Comp.* 2014; 589: 247-257.
12. Liu SR et al. Estimation of cation distribution in spinel ferrites $\text{Co}_{1+x}\text{Fe}_{2-x}\text{O}_4$ ($0.0 \leq x \leq 2.0$) using the magnetic moments measured at 10K. *Alloys and Comp.* 2013; 581: 616-624.
13. Dwivedi GD et al. Signature of ferroelectricity in magnetically ordered Mo-doped CoFe_2O_4 . *Phys. Rev. B.* 2010; 82: 134428.
14. Wang N et al. Structural and magnetic characterization of rhombohedral $\text{Ga}_{1.2}\text{Fe}_{0.8}\text{O}_3$ ceramics prepared by high-pressure synthesis. *Solid State Comm.* 2011; 151: 33-36.
15. Williamson GK and Hall WH. X-Ray Line Broadening From Fined Aluminium and Wolfram. *Acta Metall.* 1953; 1: 22-31.
16. Sanpo N et al. Microstructural and antibacterial properties of zinc-substituted cobalt ferrite nanopowders synthesized by sol-gel methods. *J. App. Phys.* 2012; 112: 084333.
17. Cesar I et al. Influence of Feature Size, Film Thickness, and Silicon Doping on the Performance of Nanostructured Hematite Photoanodes for Solar Water Splitting. *J. Phys. Chem. C* 2009; 113: 772-782.
18. Varshney D. Substitutional effect on structural and magnetic properties of $\text{A}_x\text{Co}_{1-x}\text{Fe}_2\text{O}_4$ (A = Zn, Mg and x = 0.0, 0.5) ferrites. *J. Mol. Struc.* 2011; 1006: 447-452.
19. Legodi MA and de Waal D. The preparation of magnetite, goethite, hematite and maghemite of pigment quality from mill scale iron waste. *Dyes and Pigments.* 2007; 74: 161-168.
20. Panneer MI and Bhowmik RN. Connectivity between electrical conduction and thermally activated grain size evolution in Ho-doped CoFe_2O_4 ferrite. *J. Phys. D: Appl. Phys.* 2010; 43: 465002.

21. Panda RK and Behera D. Investigation of electric transport behavior of bulk CoFe_2O_4 by complex impedance spectroscopy. *J. Alloys and Comp.* 2014; 587: 481-486.
22. Costa MM et al. Dielectric and impedance properties studies of the lead doped (PbO)-Co₂Y type hexaferrite ($\text{Ba}_2\text{Co}_2\text{Fe}_{12}\text{O}_{22}$ (Co₂Y)). *Mater. Chem. Phys.* 2010; 123: 35-39.